



저작자표시-비영리-변경금지 2.0 대한민국

이용자는 아래의 조건을 따르는 경우에 한하여 자유롭게

- 이 저작물을 복제, 배포, 전송, 전시, 공연 및 방송할 수 있습니다.

다음과 같은 조건을 따라야 합니다:



저작자표시. 귀하는 원저작자를 표시하여야 합니다.



비영리. 귀하는 이 저작물을 영리 목적으로 이용할 수 없습니다.



변경금지. 귀하는 이 저작물을 개작, 변형 또는 가공할 수 없습니다.

- 귀하는, 이 저작물의 재이용이나 배포의 경우, 이 저작물에 적용된 이용허락조건을 명확하게 나타내어야 합니다.
- 저작권자로부터 별도의 허가를 받으면 이러한 조건들은 적용되지 않습니다.

저작권법에 따른 이용자의 권리는 위의 내용에 의하여 영향을 받지 않습니다.

이것은 [이용허락규약\(Legal Code\)](#)을 이해하기 쉽게 요약한 것입니다.

[Disclaimer](#)

이학석사 학위논문

Regulation of Breast Cancer Cell
Proliferation and Metastasis
by NSDHL Mutations

2023년 2월

서울대학교 대학원
협동과정 중앙생물학과

백문주

Master' s Thesis of Science

Regulation of Breast Cancer Cell
Proliferation and Metastasis
by NSDHL Mutations

NSDHL 돌연변이에 의한
유방암 세포의 증식과 전이 조절 기능 연구

February 2023

Graduate School of Seoul National University
Interdisciplinary Programs in Cancer Biology

Moonjou Baek

Regulation of Breast Cancer Cell Proliferation and Metastasis by NSDHL Mutations

지도 교수 한 원 식

이 논문을 이학석사 학위논문으로 제출함.

2022년 10월

서울대학교 대학원
협동과정 종양생물학과
백 문 주

백문주의 이학석사 학위논문을 인준함

2023년 1월

위 원 장 임 석 아 (인)

부위원장 한 원 식 (인)

위 원 문 형 곤 (인)

Regulation of Breast Cancer Cell Proliferation and Metastasis by NSDHL Mutations

Advisor Wonshik Han

Submitting a master' s thesis

October 2022

Graduate School of Seoul National University

Interdisciplinary Programs in Cancer Biology

Moonjou Baek

Confirming the master' s thesis written by

Moonjou Baek

January 2023

Chair Seock-Ah Im (Seal)

Vice Chair Wonshik Han (Seal)

Examiner Hyeong-Gon Moon (Seal)

Abstract

Cancer cells exhibit biologically poor phenotypes induced by somatic mutations. [1, 2] Exploring the biological properties and roles of mutations related to breast cancer is a big challenge in predicting cancer risk and developing novel strategies for clinical trials. Previous studies have demonstrated that the NAD(P)-dependent steroid dehydrogenase-like (NSDHL), known to be involved in cholesterol biosynthesis in breast cancer cells, affects tumor growth and metastasis. [3-5] However, the functional changes and mechanisms of NSDHL mutations associated with malignancy in breast cancer remain unclear.

Consequently, we discovered four types of NSDHL somatic mutations in breast tumor tissues collected from patients with distant metastasis using whole-exome sequencing. Two types of NSDHL somatic mutations were selected among four types of somatic mutation, and investigated the resultant altered biological functions and the mechanisms underlying these NSDHL mutations in breast cancer.

In this study, we found that NSDHL nonsense and missense somatic

mutations enhance the proliferation, migration, and spheroid formation ability of breast cancer cells. In particular, the NSDHL nonsense mutation $\Delta 302$, induces epithelial to mesenchymal transition (EMT) and increases the EGFR expression level in vitro. We found that tumors could be rapidly and largely generated in xenograft tumor models using breast cancer cell lines expressing NSDHL somatic mutations. It was confirmed that the ability of lung metastasis was improved in the $\Delta 302$ animal model, suggesting the possible association of NSDHL somatic mutations with the malignancy of cancer cells.

Based on the experiments, two types of NSDHL somatic mutations were identified in Korean breast cancer patients with breast cancer that could induce malignancy in breast cancer. Furthermore, NSDHL gene mutations are suggested to be used as prognostic biomarkers for breast cancer patients.

Keywords : Breast cancer, NSDHL, somatic mutation, epidermal growth factor receptor (EGFR), epithelial to mesenchymal transition(EMT)

Student Number : 2021–20371

Table of contents

Abstract	i
Contents	iii
List of Tables.....	iv
List of Figures	v
I. Introduction	1
II. Materials and Methods	4
III. Results	15
IV. Discussion	40
V. References	44
Abstract – Korean.....	48

List of Tables

Table 1. Specific primer sequences used for real-time RT-PCR	10
Table 2. Information of NSDHL somatic mutations detected in the tumors of Korean patients with breast cancer	17

List of Figures

Figure 1. Lentiviral expression vector map and site of mutation in each cell line	18
Figure 2. control, WT, R60T, and Δ 302 cell lines stably expressed GFP	20
Figure 3. Proliferation ability of each cell line by proliferation assay and PI staining	22
Figure 4. Increase in the cell migration capacity of cell lines expressing NSDHL mutations.....	26
Figure 5. Enhanced spheroid formation and increased spheroid sizes due to NSDHL mutations	28
Figure 6. Promotion EMT by increasing the EMT related markers	

due to NSDHL mutations	31
Figure 7. Increase in EGFR expression due to NSDHL nonsense mutation	33
Figure 8. Enhanced tumor occurrence and growth of xenograft tumor model due to NSDHL mutations	35
Figure 9. Enhanced lung metastasis without significant change in EMT marker expression in xenograft tumor model due to NSDHL somatic mutations	38

I. Introduction

Most cancers are caused by genetic mutations; analysis of cancer-specific mutations can confirm the risk of cancer development and may be useful for diagnostic and therapeutic effects. [1, 2] Although mutation characterization is necessary to develop personalized medications for patients with cancer, an effective and easily usable system has not yet been established for this purpose; hence further studies on characterizing cancer associated gene mutations are required.

Breast cancer is the most prevalent cancer in women as well as in general population. [6, 7] The four subtypes of breast cancer include luminal A breast cancer, luminal B breast cancer, HER2-positive breast cancer, and triple-negative breast cancer (TNBC), among which, luminal types are the most common ones. [8, 9]

Epithelial-mesenchymal transition (EMT) is a cellular program that involved in carcinogenesis. [10] N-CADHERIN, SNAIL, SLUG, FIBRONECTIN, TWIST, and VIMENTIN are transcription factors and markers associated with EMT. [11, 12] During EMT, cell adhesion property of mesenchymal cells is gained, which is mediated by these transcription factors; furthermore, these cells

gain mobility and invasiveness. [13, 14]

Cholesterol plays an important role in cell growth and division by participating in membrane formation of cells and organelles. [15–17]

In most cancer cells, abnormal expression of cholesterol biosynthesis genes contributes to tumor growth and malignant progression. [18] The NAD(P) dependent steroid dehydrogenase-like (NSDHL) gene encodes sterol-4- α -carboxylate 3-dehydrogenase enzyme involved in cholesterol biosynthesis, especially in the lanosterol to cholesterol pathway. [19]

Recent studies revealed that high expression of the NSDHL gene is involved in the growth and invasiveness of breast cancer cells as well as metastasis, suggesting that this gene could be used as a diagnostic and therapeutic target. [3–5] However, the role of NSDHL mutations in breast cancer and the influences of this gene on luminal B type breast cancer have not been identified. Therefore, studying both NSDHL mutations in breast cancer and the effects of the NSDHL gene on luminal B type breast cancer is required.

In this study, we found 4 types of NSDHL somatic mutations in patients with luminal and HER2 breast cancer at Seoul National University. Among the four somatic mutations, we selected each nonsense and missense mutation that metastasized in patients with

breast cancer. We used the ZR-75-1 cell line as it is consistent with luminal B type breast cancer cell and shows a low expression of NSDHL compared to that in other breast cancer cell lines. In this study, we confirm that both missense and nonsense NSDHL mutations contribute to malignancy in patients with breast cancer. In particular, the truncated of NSDHL, generated by a nonsense mutation, induces EMT and promotes EGFR in vitro.

II. Materials and Methods

Cell lines and culture

ER+ human breast cancer cell line ZR-75-1 (KCLB No. 21500) obtained from the Korean Cell Line Bank (Seoul, Korea) was cultured on RPMI 1640 medium (WelGENE, Seoul, Korea) supplemented with 10% fetal bovine serum (FBS) and 1% penicillin-streptomycin (10,000 U/mL) (Gibco, Carlsbad, CA, USA). Cells were maintained at 37°C in a humidified atmosphere of 95% air and 5% CO₂.

Lentiviral vector construction

Lenti-c-myc-DDk-P2A-Puro vector was used for vector construction. The sequence of insert used to prepare the control vector is '5-GCGATCGCCGGCGCGCCAGATCTCAAGCTTA-ACTAGCTAGCGGACCGACGCGT-3'. Each insert of the prepared control, wild type (WT), R60T, and Δ 302 samples was inserted between Sgf1-Mlu1, a restriction site, and transformed in DH5alpha cells using the heat shock method for 1 min, followed by

cloning to the lentiviral vector construct.

Lentivirus infection

To construct control, WT, R60T, and Δ 302 cell lines, we transfected 293T cells using each vector. After 8 h of transfection, the media was replaced by the full media RPMI 1640 (WelGENE) supplemented with 10% FBS and 1% penicillin–streptomycin (Gibco). After 72 hours of transfection, 293T suspension was filtered using 0.45 μ m membrane filter, and the full media and media grown with 293T were diluted in the ratio 1:1 in a plate containing ZR-75-1 cell line. To confirm the expression of the GFP-tagged vector, we checked the GFP expression of infected ZR-75-1 cells 24 h after infection.

Puromycin selection

Cell line construction was performed using puromycin. Control, WT, R60T, and Δ 302 were all treated with RPMI 1640 (WelGENE) supplemented with 10% FBS and 1% penicillin–streptomycin (Gibco) with 4 μ g/ml of puromycin after sub-culturing for two weeks.

Cell proliferation assay

To assess cell proliferation, 3×10^3 cells were seeded in 96 well plates in each well and incubated for 24, 48, and 72h at 37 ° C. Cell proliferation abilities were evaluated using CellTiter-Glo® Luminescent Cell Viability Assay Kit (Promega, Madison, WI, USA) according to the instructions provided by the manufacturer. Luminescence was read using Luminiskan ascent (Thermo fisher scientific, Waltham, MA, USA).

Cell cycle analysis

To investigate cell cycles, 1×10^6 cells were fixed in 70% cold ethanol at 4 ° C overnight. Subsequently, 10 μ g/ml propidium iodide (PI; Sigma-Aldrich, St. Louis, USA) was added to it, and based on quantitation of DNA content, the cell cycle was analyzed using a flow cytometer (BD Bioscience, Mansfield, MA, USA). Data were analyzed using ModFit 3.0 (BD Bioscience).

Transwell migration assay

Cell migration was assessed using transwell chambers with an 8 μ m pore size insert (Falcon®). For transwell migration assay, seeded in the upper chambers at a density of 1×10^5 and the lower chambers were filled with RPMI 1640 (WeiGENE) containing 10% FBS. After incubating this experimental set up for 48 and 72h at 37 ° C, the cells migrated to the lower chamber were fixed with 4% paraformaldehyde and stained with 0.1% crystal violet solution.

Images of the stained cells were acquired using a microscope equipped with a CCD camera (Leica, Wetzlar, HE Germany). Crystal violet was then extracted with a 10% acetic acid solution, and absorbance at 540nm was read using Varioskan Lux (Thermo fisher scientific).

Wound healing assay

For the wound healing assay, 2×10^5 cells were seeded in culture-insert 2 well in μ -dish (ibidi, Munich, Germany) and incubated at 37 ° C overnight. After the cells reached 100% confluence to form a monolayer, a scratch was created on the cell

monolayer by removing the culture insert and the cells were incubated until each gap was closed. The first (0 h) and closure images (24 h and 48 h) of the gaps were acquired using a microscope equipped with a CCD camera (Leica) and the area covering the wound was measured.

Spheroid formation assay

Non-adherent three-dimensional culture, known as "spheroid formation assay," is widely used to assess the stemness of cancer cells. For spheroid formation, cells suspended in RPMI 1640 (WeiGENE) supplemented with 10% KnockOut™ Serum Replacement (Invitrogen, Carlsbad, CA, USA) and 1% penicillin-streptomycin (Gibco) were seeded at a density of 5×10^5 cells/mL on an ultra-low attachment plate coated with polymer-X. The culture medium was replaced every three days.

Quantitative reverse transcription–polymerase chain reaction (qRT–PCR)

Total RNA was extracted from cells using a Tri–RNA reagent (FAVORGEN, Kaohsiung, Taiwan). qRT–PCR was conducted using a cDNA kit (Takara, Kusatsu, Shiga, Japan). Real–time PCR reactions were run on a Light Cycler 480 II (Roche, Salt Lake City, UT, USA) using a SYBR Green PCR master mix (Applied Biosystems) and specific primers (Table 1). Results were analyzed using the Δ CT method or $2^{-\Delta\Delta$ CT method, which reflects the threshold difference between a target gene and GAPDH in each sample, as well as the relative gene expression, with the reference sample set to 1 (control).

Table 1. Specific primer sequences used for real-time RT-PCR

Gene	Sequence (5'→3')	
NSDHL	Forward	GGTGACGCACAGTGGAAAAC
	Reverse	TCGCACGGACTCATTTGACA
E-CADHERIN	Forward	ATTCTGATTCTGCTGCTCTT
	Reverse	AGTAGTCATAGTCCTGGTCT
N-CADHERIN	Forward	CTCCTATGAGTGGAACAGGAACG
	Reverse	TTGGATCAATGTCATAATCAAGTGCTGTA
SNAIL	Forward	GAGGCGGTGGCAGACTAG
	Reverse	GACACATCGGTCAGAGGT
SLUG	Forward	CATGCCTGTCATAACCACAAC
	Reverse	GGTGTCTCAGATGGAGGAGGG
VIMENTIN	Forward	CCCTCACCTGTGAAGTGGAT
	Reverse	TCCAGCAGCTTCCTGTAGGT
TWIST	Forward	CGGGAGTCCGCAGTCTTA
	Reverse	TGAATCTTGCTCAGCTTGTC
FIBRONECTIN	Forward	CAGAATCCAAGCGGAGAGAG
	Reverse	CATCCTCAGGGCTCGAGTAG
GAPDH	Forward	GAGTCCAGGGCGTCTTCA
	Reverse	GGGGTGCTAAGCAGTTGGT

Western blotting

For western blotting, cells were lysed in RIPA buffer (Sigma, St. Louis, MO, USA). Proteins were separated using SDS-PAGE and transferred onto Immobilon-P Transfer membranes (Merck Millipore, Bedford, MA, USA). After blocking with 5% BSA in TBS-T at room temperature for 1 h and 30min, the membrane was incubated with primary antibodies (β -actin [1:2000], NSDHL [1:10000] E-CADHERIN [1:1000], N-CADHERIN [1:1000], SNAIL [1:2000], SLUG [1:2000], EGFR [1:1000]) overnight at 4°C and horseradish peroxidase-conjugated secondary antibodies at room temperature for 1 h and visualized using SuperSignal West Pico Chemiluminescent Substrate (Thermo Fisher Scientific) and Amersham Imager 600 (GE Healthcare, Buckinghamshire, UK). The relative intensities of the bands observed by western blotting were analyzed using ImageJ software (National Institutes of Health, Bethesda, MD, USA).

Immunofluorescent staining

Cells were fixed with 4% paraformaldehyde, permeabilized using 1%

BSA/PBS– Triton X–100 at 4°C, and incubated with primary antibodies at appropriate ratios (NSDHL [1:10000], E–CADHERIN [1:1000], N–CADHERIN [1:200], SNAIL [1:500], SLUG [1:200] and EGFR [1:300]) overnight at 4°C and secondary antibodies (Alexa Fluor® 594 goat anti–rabbit IgG (H+L) [1:500] at room temperature for 30 min, followed by incubation with NucBlue® Live REAdyProbes™ REAgent (Thermo Fisher Scientific). The cell images were acquired using a confocal microscope (Leica).

Xenograft animal model

NOD.Cg–Prkdcscid Il2rgtm1wjl /SzJ mice (NSG mice) were obtained from The Jackson Laboratory (Bar Harbor, ME, USA). All animal experiments were approved by the Institutional Animal Care and Use Committee of the Seoul National University (IACUC, SNU 200907–4). A total of twenty–four female NSG mice were used in this study. Orthotopic xenografts were established by injecting 5×10^6 cells of Parent, WT, R60T and $\Delta 302$ –cells mixed with Matrigel (BD Biosciences) into the fat pad of the fourth mammary

gland of 6-weeks old mice and allowed to drink water supplemented with β -estradiol (6.25 $\mu\text{g}/\text{ml}$). After injection of tumor cells, the primary tumor volume was measured twice a week using digital calipers and a modified ellipsoidal formula (volume= $1/2$ [length \times width 2]).

Immunohistochemistry

The primary tumors were fixed with 4% buffered paraformaldehyde, embedded in paraffin blocks, and sectioned into 4- μm thick sections. The sections were deparaffinized using xylene, rehydrated using serially diluted ethanol, and pretreated with citric acid (pH 6.0) by autoclaving at 95°C for 20 min for antigen retrieval. Endogenous peroxidase activity was blocked by incubating the samples with 3% H_2O_2 for 10 min at room temperature. After incubation with 10% normal goat serum for 1 h to block nonspecific binding of immunological reagents, samples were incubated with primary antibodies at 4°C overnight and exposed to secondary antibodies. Subsequently, the samples were stained using the DAB

chromogen kit (Agilent Technologies, Glostrup, Denmark) and the immunoreaction was visualized. Nuclei were counterstained with hematoxylin solution (Merck Millipore, Burlington, MA) according to the instructions provided by the manufacturer. Histological images of the stained tissues were acquired using a microscope equipped with a CCD camera (Leica).

Statistical analysis

Data obtained from all in vitro and in vivo analysis, are presented as mean \pm standard deviation of at least three independent experimental repeats. Statistical comparisons between two independent groups were performed using unpaired t-tests. For groups of three or more, data were compared using Kruskal–Wallis nonparametric ANOVA followed by Dunn's multiple comparison tests. Statistical analyses were performed using GraphPad Prism v9.2.0 (GraphPad Software Inc., La Jolla, CA, USA). Statistical significance was considered at $P < 0.05$.

III. Results

Identification of NSDHL gene mutation from tissues of Korean patients with breast cancer

Using whole exome sequencing of tumor tissues from Korean patients with breast cancer at Seoul National University Hospital, we identified three missense and 1 nonsense somatic mutation of NSDHL involved in cholesterol biosynthesis (Table 2).

Cancer recurrences in the lung, brain, and bone were found after surgery in patients carrying Mutant 2 and 4.

NSDHL Mutant 1 (K38R), identified in two patients with breast cancer, is a point mutation at the co-factor binding region. NSDHL Mutant 2 (R60T) detected in only one patient with breast cancer is another point mutation in the co-factor binding site. NSDHL Mutant 3 (R119K) and Mutant 4 (Δ 302), identified in one patient with breast cancer each, represent point mutations at the catalytic domain site and the transmembrane helix region, respectively.

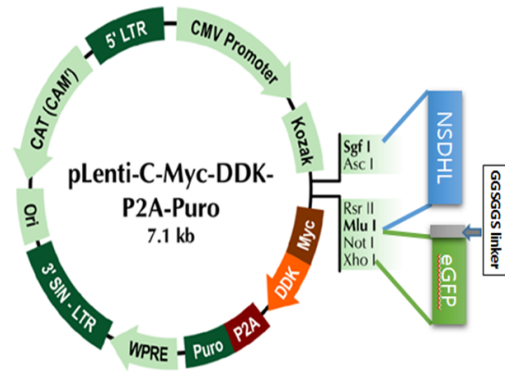
The R60T used in the study is a missense mutation and is characterized by the 60th amino acid arginine of NSDHL replaced

by thymine. Unlike other NSDHL mutations, $\Delta 302$ is a nonsense mutation, in which part of NSDHL c-terminal is truncated and the transmembrane is not fully transcribed.

Table 2. Information of NSDHL somatic mutations detected in the tumors of Korean patients with breast cancer

NSDHL Mutant	#chr_name	chr_start	Frequency	Surgical specimen (IHC)				Region	Mutation type	Base mutation	Protein change	Mutational region of NSDHL
				ER(%)	PR(%)	HER2	Ki67(%)					
Mutant 1	chrX	152018813	2	Positive	Negative	Positive	20	exonic	Nonsynonymous_SNV (missense mutation)	A113G	K38R	near co-factor binding site (V44-D68)
				Negative	Negative	Positive (+++)	10					
Mutant 2	chrX	152018879	1	Negative	Negative	Positive (+++)	15	exonic	Nonsynonymous_SNV (missense mutation)	G179C	R60T	co-factor binding site (V44-D68)
Mutant 3	chrX	152027402	1	Negative	Negative	++	10	exonic	Nonsynonymous_SNV (missense mutation)	G356A	R119K	Near Catalytic site (Y172 K176)
Mutant 4	chrX	152037444	1	Positive	Negative	Positive	10	exonic	Stopgain_SNV (nonsense mutation)	C906A	Y302X	Transmembrane helix region (Y297-P316)

A



B

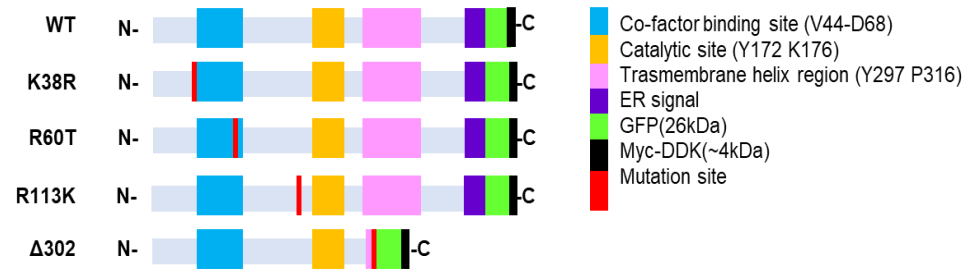


Figure 1. Lentiviral expression vector map and site of mutation in each cell line

Establishment of the cell lines stably expressing NSDHL nonsense and missense mutations

GFP-expression vectors were used for constructing the control, WT, R60T, and Δ 302 cell lines (Figure 1). Thus, the establishment of cell lines was confirmed by the GFP expression. We investigated the GFP expression in each cell line based on the fact that the ZR-75-1 Parent which was not infected with lentivirus, did not express GFP. FACs analysis revealed that, lentivirus infected control, WT, R60T, and Δ 302 cells expressed more than 95% of GFP compared to that detected in Parent cell line (Figure 2A). By immunofluorescence staining, we confirmed that GFP was expressed in control, WT, R60T and Δ 302 cell lines (Figure 2C). Moreover, during western blotting, exogenous NSDHL protein expression was found in control, WT, R60T and Δ 302 cell lines, but not in the Parent and control (Figure 2B).

These results suggest that the gene present in the vector was successfully expressed in ZR-75-1; thus control, WT, R60T, and Δ 302 cell lines were successfully constructed.

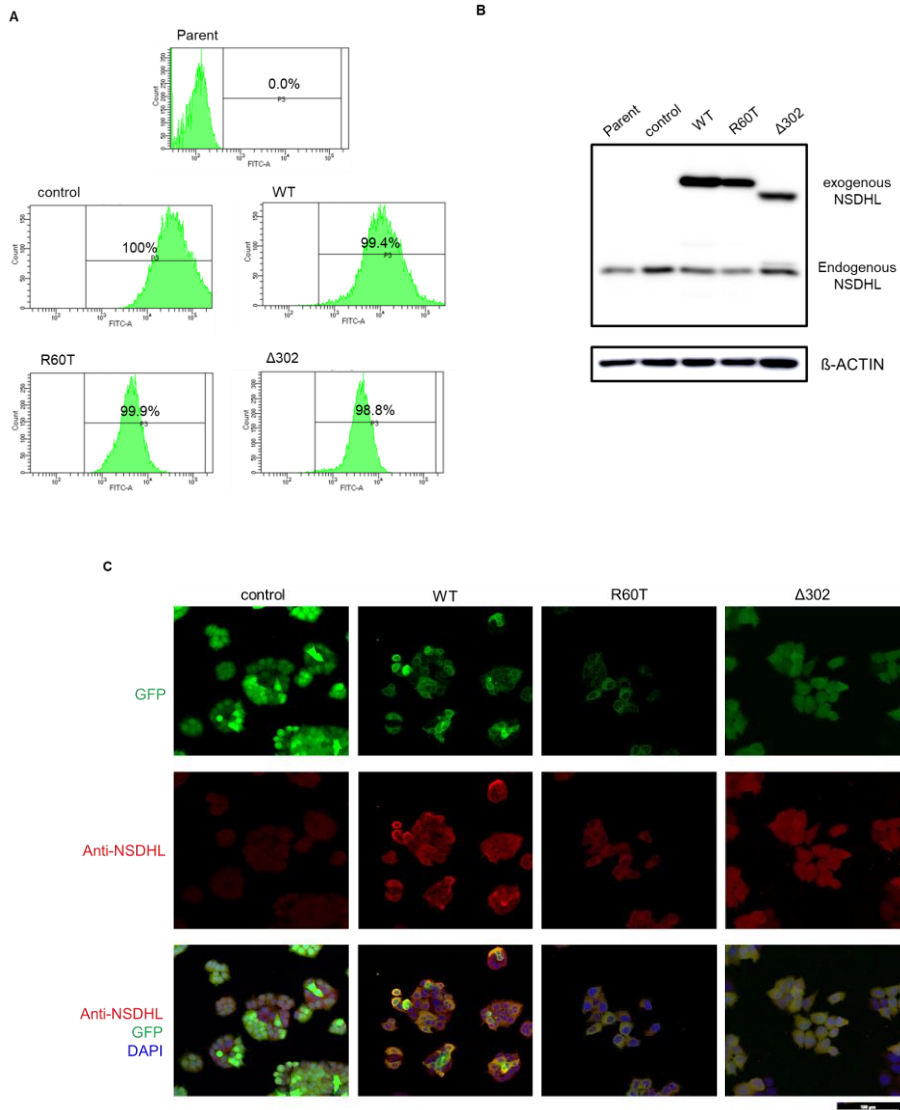


Figure 2. Control, WT, R60T, and $\Delta 302$ cell lines stably expressed GFP **A.** Percentages of GFP positive cells were more than 95% in control, WT, R60T, and $\Delta 302$. **B.** GFP and NSDHL expression were detected using Western blotting. **C.** GFP and NSDHL expression in control, WT, R60T, and $\Delta 302$ detected using immunofluorescence staining.

NSDHL nonsense and missense mutations enhanced the proliferative capacity of ZR-75-1.

To compare the proliferative capacity of ZR-75-1 cells by NSDHL mutations, CellTiter-Glo assay was performed at intervals of 24 hours for 3 days and cell cycle was assessed using PI staining.

No significant change was observed in WT, which is the NSDHL overexpressing cell line, compared with that in control. (Figure 3A). Similarly, cell cycle assay using PI staining indicated that, S and G2/M phases, indicative of cell proliferation, did not differ significantly between the WT and control sets (Figure 3B). However, the CellTiter-Glo assay, revealed enhanced proliferation ability of the mutant cell lines, R60T and Δ 302, compared with that in control and WT (Figure 3A).

These results suggest that NSDHL overexpression could not alter cell proliferation in ZR-75-1 cells, which is one of the luminal B type breast cancer cell lines. However, both NSDHL nonsense and missense gene mutations such as R60T and Δ 302 were involved in the enhancement of cell proliferation in breast cancer.

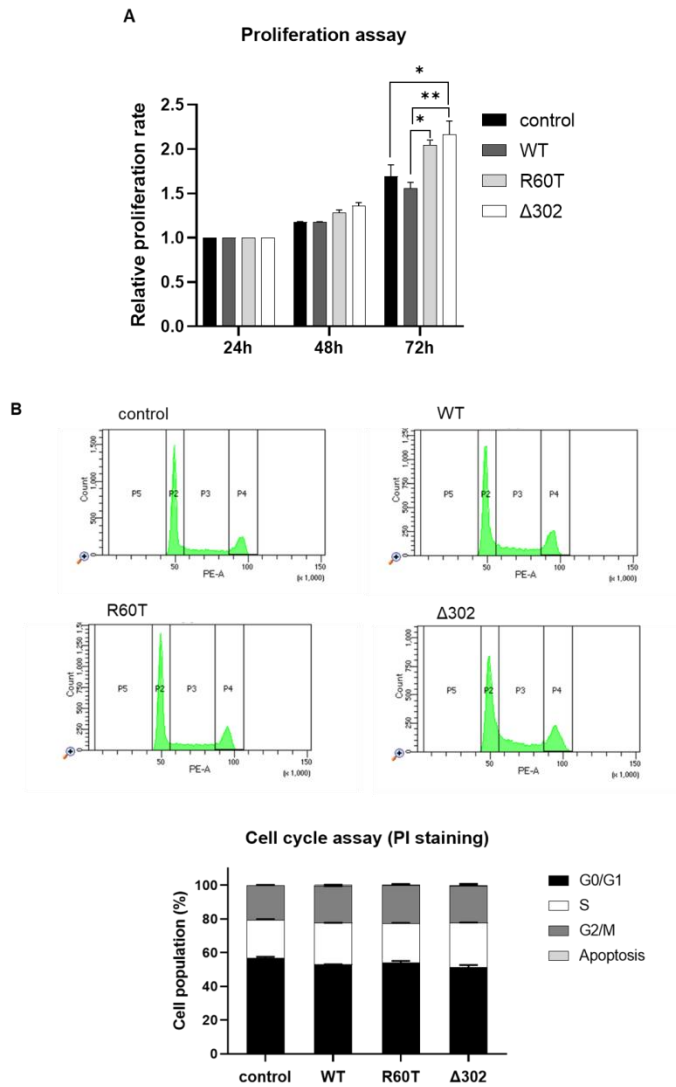


Figure 3. Proliferation ability of each cell lines by proliferation assay and PI staining

A. Proliferation assay of the different ZR-75-1 stable cell lines to confirm growth. B. Cell cycle analysis to evaluate althered cell proliferation capacity.

NSDHL nonsense and missense mutations promoted the migration ability of ZR-75-1

Transwell migration and wound healing assays were performed to investigate changes in the migration ability of ZR-75-1 induced by NSDHL nonsense and missense mutations.

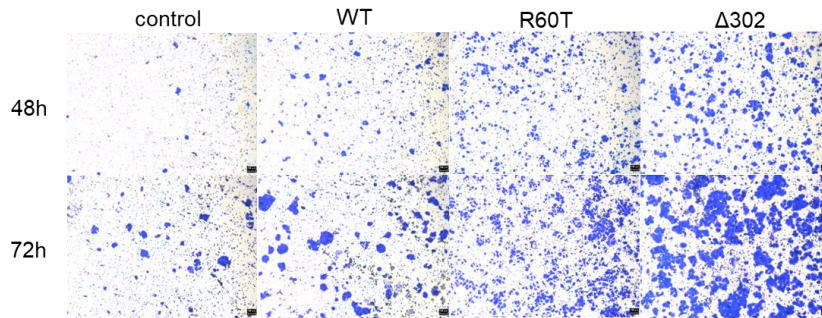
After 48 and 72 h of transwell migration, the WT (NSDHL gene overexpressed) cell lines did not show enhancement in cell migration ability compared to that in the control. However, R60T and Δ 302 cell lines showed improved cell migration ability than that of WT. In particular, Δ 302 that expresses NSDHL nonsense mutation, showed the highest migration capacity compared with WT and R60T. (Figure 4 A, B)

Similarly, wound healing assay for three days at 24 h intervals revealed increased migration ability of WT cells compared with that for control; migration capacity was greater in R60T and Δ 302 than in WT cells. The migration ability of Δ 302 was particularly improved. (Figure 4 C, D)

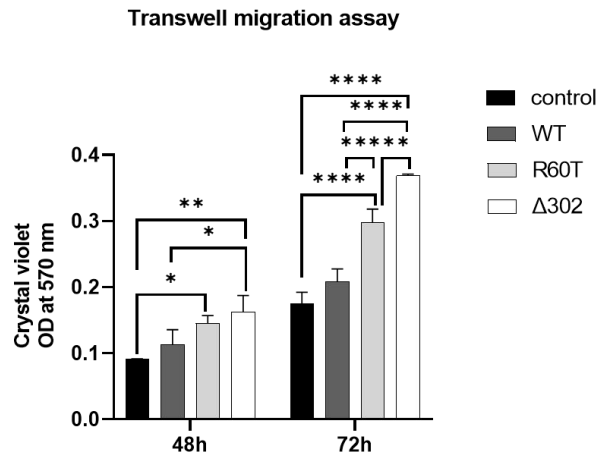
These results suggest the possible involvement of the NSDHL gene

mutations like R60T and Δ 302 behind the mechanisms of improved migration of breast cancer cells.

A



B



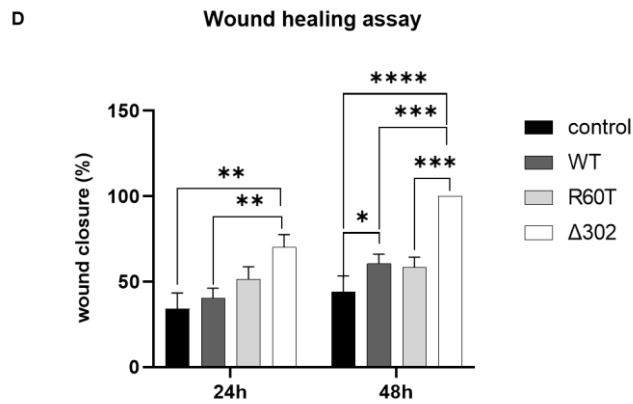
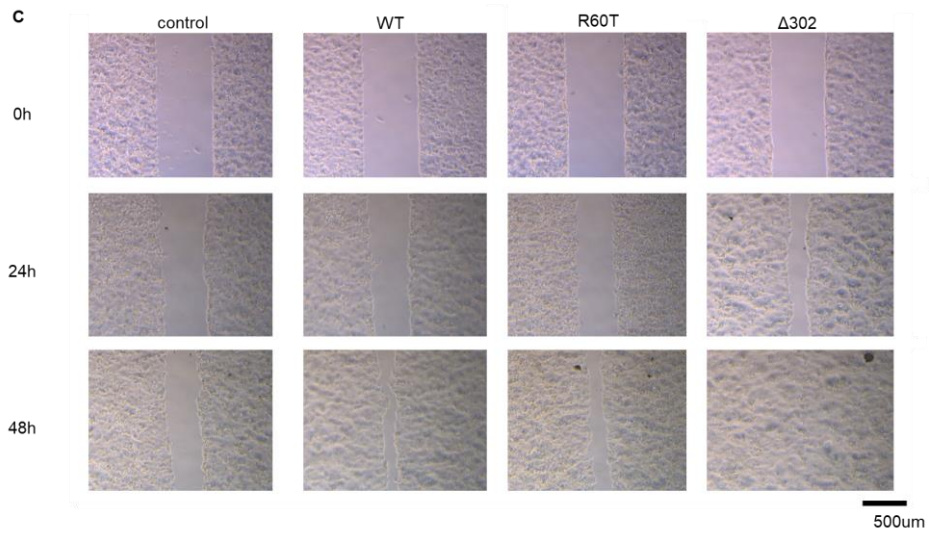


Figure 4. Increase in the cell migration capacity of cell lines expressing NSDHL mutations

A, B, C, D. Relative images and analyses results of the transwell migration and wound healing assays of each cell line. * $P < 0.05$, ** $0.001 < P < 0.05$, **** $P < 0.0001$

NSDHL nonsense and missense mutation improved tumor spheroid formation in ZR-75-1 cultured on the ultra-low attachment plate

Spheroid formation is related to the characteristics of cancer stem cells and is involved in cancer metastasis and recurrence. [19, 20] We performed a spheroid formation assay to analyze the correlation between the spheroid formation ability and NSDHL somatic mutations. When observed for 48 and 72 h, large spheroids were formed in R60T and Δ 302 (Figure 5 A, B). The percentage of spheroids with diameters larger than 100 μ m was more than 50 in both R60T and Δ 302 cell lines (Figure 5 C). Moreover, more compact shapes of spheroids were observed in R60T and Δ 302 than in control and WT cells. (Figure 5 A, B)

These results result indicate that NSDHL gene mutations such as R60T and Δ 302 enhance breast cancer stem cell characteristics promoting breast cancer metastasis and recurrence.

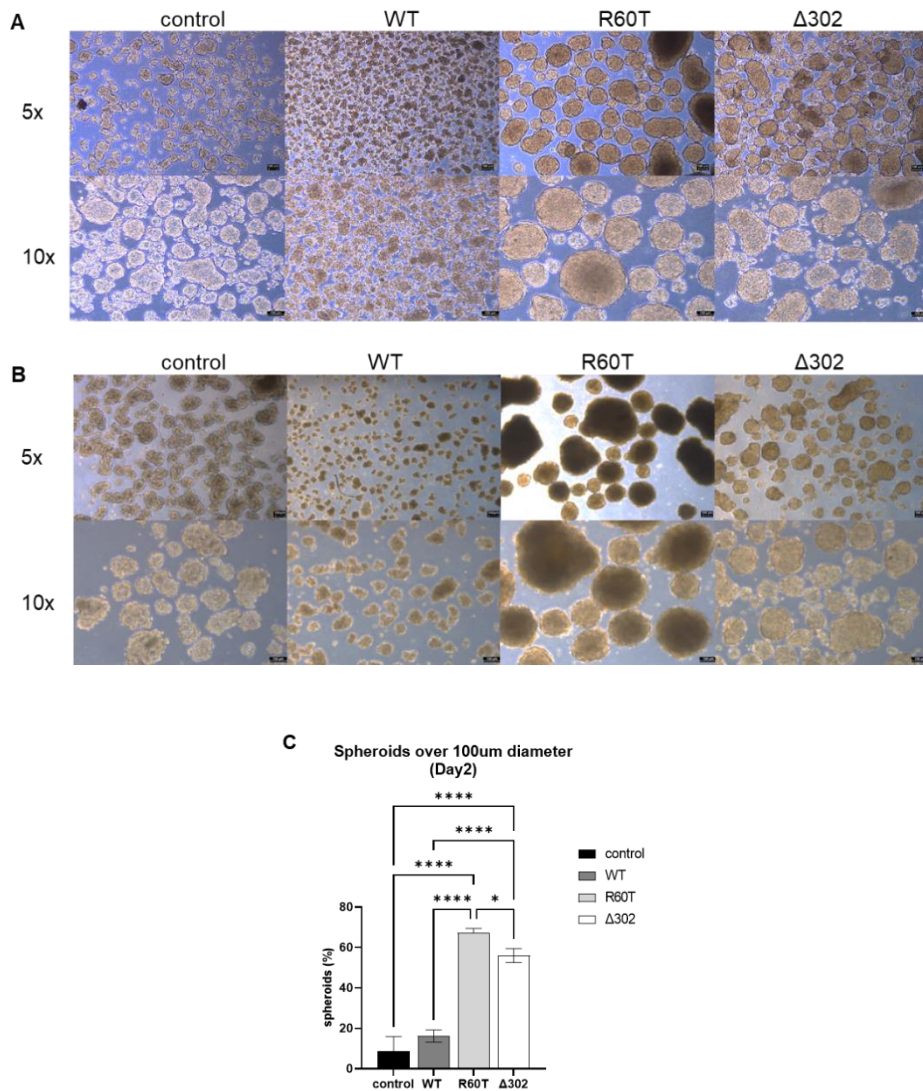


Figure 5. Enhanced spheroid formation and increased spheroid sizes due to NSDHL mutations A, B. Spheroid formation ability of control, WT, R60T and Δ 302 cells after 48 and 72 h of spheroid formation assay. C. Comparison of spheroid sizes larger than 100 um diameter after two days of spheroid formation assay. * $P < 0.05$,

0.0001<P<0.001, *P<0.0001

Somatic mutations in NSDHL gene regulated the epithelial to mesenchymal transition (EMT) marker of ZR-75-1 cell lines

To examine EMT in the metastatic stage of cancer, mRNA and protein expression levels of EMT markers were investigated. [10, 11] Expression levels of the mesenchymal cell markers N-CADHERIN, SNAIL, and SLUG, were analyzed.

Both qRT-PCR and western blotting revealed higher expression of N-CADHERIN, SNAIL and SLUG in $\Delta 302$ than in WT and R60T cells (Figure 6). Protein expression levels of E-CADHERIN, which has a role in mesenchymal epithelial transition (MET), was reduced in R60T and $\Delta 302$ than in WT cells. (Figure 6 B)

The results of this study suggest both missense and nonsense mutations in NSDHL such as R60T and $\Delta 302$, respectively, that cause an increase in the expression of the mesenchymal markers and induce EMT.

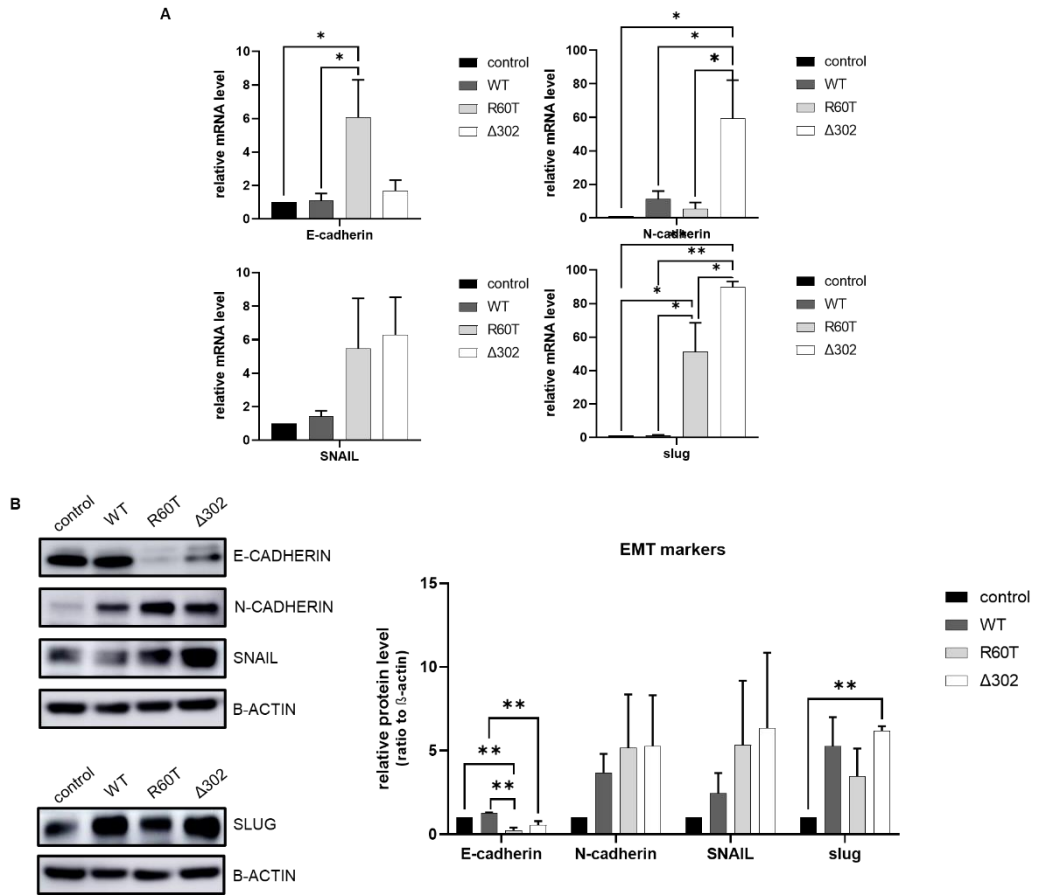


Figure 6. Promotion EMT by increasing the EMT-related markers due to NSDHL mutations

A. EMT marker expression levels evaluated by qRT-PCR. B. EMT marker expression levels evaluated using Western blotting.

* $P < 0.05$, ** $0.001 < P < 0.05$

NSDHL nonsense mutation increased epidermal growth factor receptor (EGFR) expression

To examine the effect of NSDHL gene mutations on the malignancy of ZR-75-1, the expression changes in EGFR, which cause basal-like characteristics in breast cancer cells, were confirmed. [21] The expression levels of EGFR protein indicated, that $\Delta 302$ cell line with NSDHL nonsense mutation showed higher EGFR expression than in control (Figure 7).

In breast cancer, high expression of EGFR is known to promote malignancy. Hence, this result suggests that the enhanced migration ability of $\Delta 302$ cell EGFR signaling.

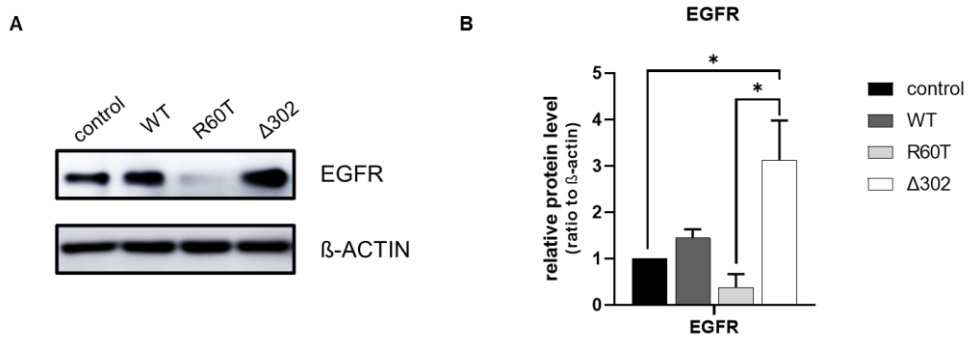


Figure 7. Increase in EGFR expression due to *NSDHL* nonsense mutations

A, B. Representative western blotting image and relative expression levels of EGFR in control, WT, R60T, and Δ 302 cells. * $P < 0.05$

Mutations in NSDHL promoted tumor occurrence and growth of xenograft tumor models

Compared to the tumor growth in the Parent and WT xenograft tumor models, tumors were formed more rapidly in R60T and Δ 302 models. Moreover, the sizes of tumors in R60T and Δ 302 models were bigger than that in WT (Figure 8 B). Particularly, tumor formation and growth in Δ 302 were significantly faster than that of other xenograft tumor models (Figure 8 A).

Thus, R60T and Δ 302 mutations in NSDHL may promote tumorigenesis and growth.

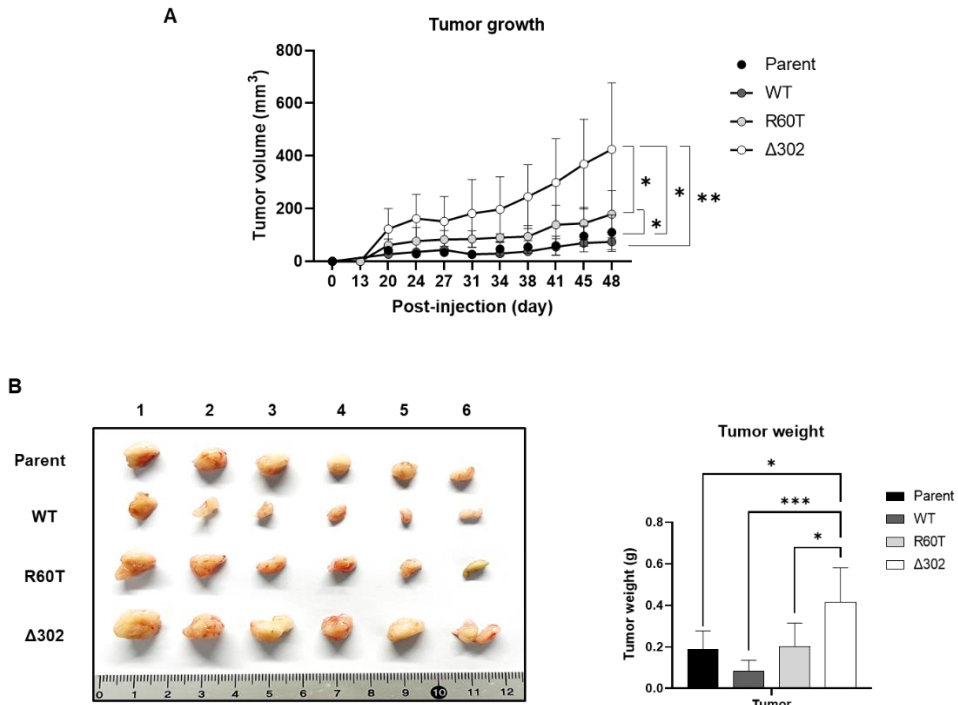


Figure 8. Enhanced tumor occurrence and growth of xenograft tumor model due to *NSDHL* mutations

A. Graph of tumor growth in Parent, WT, R60T and $\Delta 302$ models recorded twice a week. **B.** Representative gross image and graph of tumor weight in Parent, WT, R60T and $\Delta 302$ models. * $P < 0.05$, ** $0.001 < P < 0.05$ *** $0.0001 < P < 0.001$

NSDHL nonsense mutation enhanced metastasis in xenograft tumor models

To confirm the metastatic effect of mutations and overexpression of the NSDHL, the xenograft tumor models were sacrificed 60 days after transplantation of ZR-75-1 cell lines and their lungs were excised (Figure 9A). Lung metastasis was analyzed using H&E staining and HLA immunohistochemistry. We found that 1 out of 6 in the Parent, 4 out of 6 in the WT, 3 out of 6 in the R60T and all 6 mice in the $\Delta 302$ xenograft tumor models had lung metastasis. By measuring the areas of lung metastasis, we confirmed that metastasis occurred more sporadically in $\Delta 302$ xenograft tumor models than in other xenograft tumor models (Figure 9B, C).

Among the xenograft tumor models, $\Delta 302$ showed the most enhanced lung metastasis; hence, NSDHL nonsense mutations like $\Delta 302$ can be considered to promote metastasis.

Mutations in NSDHL showed no significant change in the expression levels of EMT markers in the tumors of xenograft models

Our in vitro assay, confirmed the expression of EMT markers in the Parent, WT, R60T and Δ 302 xenograft tumor models.

We confirmed that the EMT markers, N-CADHERIN and SNAIL induced no significant change in the tumors of R60T and Δ 302 xenograft models (Figure 9D).

This suggests that NSDHL mutations in both the R60T and Δ 302 models do not produce any significant effect on EMT.

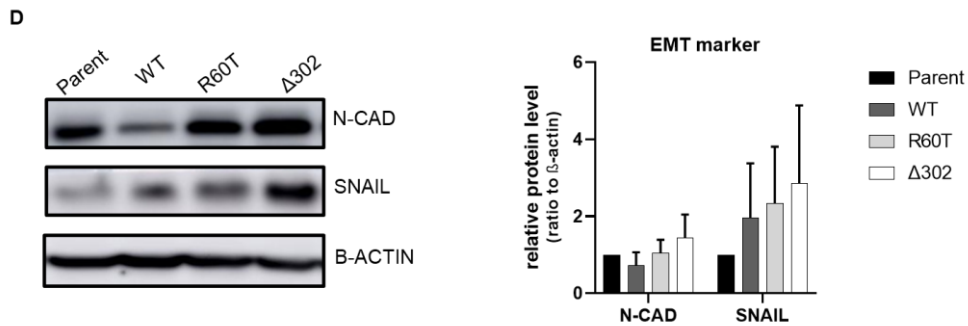


Figure 9. Enhanced lung metastasis without significant change in EMT marker expression in xenograft tumor model due to *NSDHL* somatic mutations.

A, B. Images of lungs and graph showing the number of lung metastasis foci. C. Results of immune-histological analyses of lung metastasis D. Representative Western blotting images of N-CADHERIN and SNAIL in xenograft tumor and their quantification data. ****P<0.0001

IV. Discussion

Cholesterol is a unique lipid essential for cell proliferation and differentiation. [18] Most cancer cells show abnormal cholesterol production and metabolic processes, leading to high intracellular cholesterol levels. [20]

NSDLH involved in cholesterol biosynthesis, affect the localization and trafficking of membrane-binding proteins. [19] These proteins regulate cell survival, migration and invasion through localization of signaling proteins. In TNBC, high expression of NSDHL promotes cancer cell growth, migration, and invasion through EGFR and TGF- β / SMAD signaling. Further, NSDHL increases cell sensitivity to EGFR-targeted drugs such as erlotinib, promotes lung metastasis, and is a poor prognostic factor associated with recurrence of cancer. [3-5]

Despite the malignancy -associated feature of NSDHL, it's mutations in breast cancer were not identified. Therefore, studying the mechanisms and altered functional impact of NSDHL mutations on breast cancer is crucial.

In this study, luminal B type ZR-75-1 cells with relatively low

expression of *NSDHL* were used; the effects of NSDHL have not yet been studied in different breast cancer subtypes. [21] To identify the effects of the NSDHL somatic mutations, WT NSDHL overexpressing cell lines, as well as NSDHL nonsense and missense mutation-expressing cell lines R60T and Δ 302, were established.

NSDHL overexpressing WT cell line showed no change in functional impacts or EMT-related marker expression levels compared with those in control. However, NSDHL missense and nonsense mutations R60T and Δ 302, enhanced not only proliferation and migration abilities but also spheroid formation ability of ZR-75-1 cells. The tumor formation was accelerated in the mutant xenograft tumor models. Moreover, when Δ 302, NSDHL nonsense mutation, was expressed, EMT markers and displayed lung metastasis capacity that were higher than in WT.

According to the study, overexpression of NSDHL possibly had no effects on the ZR-75-1 cell proliferation and luminal B type breast cancer cell line; NSDHL somatic mutations, especially Δ 302, may

contribute to the malignancy of the breast cancer.

First, NSDHL-overexpressing WT ZR-75-1 cell line showed no significant functional or mechanism-associated changes compared with the control. Considering these results, the overexpression of NSDHL may not significantly affect the malignancy in luminal B type breast cancer cells.

In the case of R60T, a type of NSDHL missense mutation, enhanced proliferation and migration abilities were noticed, but the expression of EGFR, usually high in basal-like and TNBC subtypes, was reduced. Therefore, studies on other mechanisms related to proliferation and migration abilities changes are needed.

CHILD syndrome is caused by mutations in NSDHL that results in impaired cholesterol or sterol synthesis or accumulation of intermediates produced by NSDHL. According to previous reports, among the NSDHL mutations causing CHILD syndrome, nonsense mutations that induce truncated C-terminal regions, which results in proteins that are not trapped from the Golgi apparatus to the endoplasmic reticulum, atypically present in the cytoplasm. This phenomenon eventually contributes to the malignancy in CHILD syndrome by interfering with fat droplet formation. [22-24]

Similarly, in immunofluorescence staining analysis results, NSDHL was atypically present in the cytoplasm in the case of $\Delta 302$, a nonsense mutation rather than in cases of control, WT, and R60T. Considering that the expression of NSDHL is widely distributed in the cytoplasm of the $\Delta 302$ cell line, suggesting that nonsense mutations such as $\Delta 302$ may contribute to the malignancy of breast cancer cells. So, further studies about the effects of the cytoplasmic distribution of NSDHL involving nonsense mutation are needed.

In this study, we focused only on the functional changes of breast cancer cells and the expression patterns of EMT markers and EGFR, but the details of pathways remain to be explored. So, further studies can reveal the comprehensive knowledge on mechanisms related to the improvement of their ability.

V. References

1. Balmain, A., The critical roles of somatic mutations and environmental tumor-promoting agents in cancer risk. *Nat Genet*, 2020. **52**(11): p. 1139–1143.
2. Luzzatto, L., Somatic mutations in cancer development. *Environ Health*, 2011. **10 Suppl 1**: p. S12.
3. Chen, M., et al., NSDHL promotes triple-negative breast cancer metastasis through the TGFbeta signaling pathway and cholesterol biosynthesis. *Breast Cancer Res Treat*, 2021. **187**(2): p. 349–362.
4. Yoon, S.H., et al., NSDHL knockdown decreases tightly cohesive tumorsphere formation and breast cancer stem cell population. *Cancer Research*, 2022. **82**(4).
5. Yoon, S.H., et al., NAD(P)-dependent steroid dehydrogenase-like is involved in breast cancer cell growth and metastasis. *BMC Cancer*, 2020. **20**(1): p. 375.
6. Sung, H., et al., Global Cancer Statistics 2020: GLOBOCAN Estimates of Incidence and Mortality Worldwide for 36 Cancers in 185 Countries. *CA Cancer J Clin*, 2021. **71**(3): p. 209–249.

7. Arnold, M., et al., Current and future burden of breast cancer: Global statistics for 2020 and 2040. *Breast*, 2022. **66**: p. 15–23.
8. Dai, X.F., et al., Breast cancer intrinsic subtype classification, clinical use and future trends. *American Journal of Cancer Research*, 2015. **5**(10): p. 2929–2943.
9. Yersal, O. and S. Barutca, Biological subtypes of breast cancer: Prognostic and therapeutic implications. *World J Clin Oncol*, 2014. **5**(3): p. 412–24.
10. Chen, T., et al., Epithelial–mesenchymal transition (EMT): A biological process in the development, stem cell differentiation, and tumorigenesis. *J Cell Physiol*, 2017. **232**(12): p. 3261–3272.
11. Goossens, S., et al., EMT transcription factors in cancer development re–evaluated: Beyond EMT and MET. *Biochim Biophys Acta Rev Cancer*, 2017. **1868**(2): p. 584–591.
12. Grzegorzolka, J., et al., Expression of EMT Markers SLUG and TWIST in Breast Cancer. *Anticancer Res*, 2015. **35**(7): p. 3961–8.
13. Huang, Y., W. Hong, and X. Wei, The molecular mechanisms

and therapeutic strategies of EMT in tumor progression and metastasis. *J Hematol Oncol*, 2022. **15**(1): p. 129.

14. Tania, M., M.A. Khan, and J. Fu, Epithelial to mesenchymal transition inducing transcription factors and metastatic cancer. *Tumour Biol*, 2014. **35**(8): p. 7335–42.
15. Chen, H.W., H.J. Heiniger, and A.A. Kandutsch, Relationship between Sterol Synthesis and DNA–Synthesis in Phytohemagglutinin–Stimulated Mouse Lymphocytes. *Proceedings of the National Academy of Sciences of the United States of America*, 1975. **72**(5): p. 1950–1954.
16. Chen, H.W., A.A. Kandutsch, and C. Waymouth, Inhibition of cell growth by oxygenated derivatives of cholesterol. *Nature*, 1974. **251**(5474): p. 419–21.
17. Martinez–Botas, J., et al., Dose–dependent effects of lovastatin on cell cycle progression. Distinct requirement of cholesterol and non–sterol mevalonate derivatives. *Biochimica Et Biophysica Acta–Molecular and Cell Biology of Lipids*, 2001. **1532**(3): p. 185–194.
18. Kuzu, O.F., M.A. Noory, and G.P. Robertson, The Role of Cholesterol in Cancer. *Cancer Res*, 2016. **76**(8): p. 2063–70.

19. Gabitova, L., A. Gorin, and I. Astsaturov, Molecular pathways: sterols and receptor signaling in cancer. *Clin Cancer Res*, 2014. **20**(1): p. 28–34.
20. Sawada, M.I., S.F. GD, and M. Passarelli, Cholesterol derivatives and breast cancer: oxysterols driving tumor growth and metastasis. *Biomark Med*, 2020. **14**(14): p. 1299–1302.
21. Holliday, D.L. and V. Speirs, Choosing the right cell line for breast cancer research. *Breast Cancer Res*, 2011. **13**(4): p. 215.
22. Yang, Z., et al., Large deletions in the NSDHL gene in two patients with CHILD syndrome. *Acta Derm Venereol*, 2015. **95**(8): p. 1007–8.
23. du Souich, C., et al., *NSDHL-Related Disorders*, in *GeneReviews((R))*, M.P. Adam, et al., Editors. 1993: Seattle (WA).
24. Getz, G.I., et al., *Identification of NSDHL mutations associated with CHILD syndrome in oral verruciform xanthoma*. *Oral Surg Oral Med Oral Pathol Oral Radiol*, 2019. **128**(1): p. 60–69.

국문 초록

체세포 돌연변이는 암세포에 생물학적으로 나쁜 표현형을 갖도록 한다. 유방암에서 유전자 돌연변이에 대한 생물학적 특성과 기능 연구는 암 발생을 예측하고, 임상시험에서 새로운 전략을 개발하는데 있어서 큰 도전이다.

유방암 세포에서 콜레스테롤 생합성에 관여한다고 알려진 NSDHL 유전자는 종양의 성장 및 전이에 영향을 미친다는 연구들이 있지만, 돌연변이에 의한 세포의 기능 변화 및 기전에 대하여는 아직 알려진 바 없다. 따라서 우리는 유방암 환자의 종양 조직으로부터 Whole-exome sequencing을 통해 NSDHL 유전자의 4가지 체세포 돌연변이를 발견하였다. 이 중 2가지 체세포 돌연변이를 선택하여 NSDHL 돌연변이체에 의한 유방암 세포의 생물학적 특성의 변화 및 관련 기전에 대하여 알아보고자 하였다.

본 연구를 통하여 NSDHL의 nonsense, missense 체세포 돌연변이는 유방암 세포의 증식 및 이동 능력을 증가시킬 뿐 아니라 스페로이드 형성 능력을 향상시키는데 기여함을 확인하였다. 특히 $\Delta 302$ 와 같은 NSDHL nonsense 돌연변이는 유방암 세포에서 상피-간엽 전이를 유도

하고 표피 성장 인자 수용체의 발현을 증가시킴을 규명하였다. 뿐만 아니라 동물 실험을 통하여 NSDHL 돌연변이를 발현하는 유방암 세포주를 이용하여 만든 동물모델에서 종양이 빠르고 크게 생성되었음을 확인하였다. 특히 NSDHL nonsense 돌연변이인 $\Delta 302$ 동물 모델의 경우 폐로의 전이 능력이 향상됨을 확인함으로써 NSDHL 돌연변이가 암세포의 악성화에 기여할 것이라는 가능성을 제시하였다.

따라서 본 결과를 토대로 한국인 유방암 환자로부터 확인할 수 있었던 두 가지 유형의 NSDHL 체세포 돌연변이가 유방암의 악성화에 기여할 것으로 생각된다. 더하여 NSDHL 돌연변이 유전자는 유방암 환자의 예후 예측의 바이오마커로 활용될 수 있을 것이라고 생각된다.

주요어 : 유방암, NSDHL, 체세포 돌연변이, 상피-간엽 전이, 표피 성장 인자 수용체

학번 : 2021-20371